

AAEC/E399



INIS.  
TRN AU7703582

AAEC/E399

AUSTRALIAN ATOMIC ENERGY COMMISSION  
RESEARCH ESTABLISHMENT  
LUCAS HEIGHTS

NEUTRON ENERGY SPECTRA FROM THE THICK TARGET  
 ${}^9\text{Be}(d,n){}^{10}\text{B}$  REACTION

by

S. WHITTLESTONE

December 1976  
ISBN 0 642 99764 0

AUSTRALIAN ATOMIC ENERGY COMMISSION  
RESEARCH ESTABLISHMENT  
LUCAS HEIGHTS

NEUTRON ENERGY SPECTRA FROM THE THICK TARGET  
 ${}^9\text{Be}(d,n){}^{10}\text{B}$  REACTION

by

S. WHITTLESTONE

ABSTRACT

The energy spectrum of neutrons emitted when deuterons impinge on a thick beryllium target has been measured using an NE213 scintillation detector and the time-of-flight technique. Spectra were measured at angles of 0, 30, 45, 60, 90, 120 and 150° for deuteron energies of 1.4, 1.8, 2.3 and 2.8 MeV. Tables are presented of these angle-dependent energy spectra, the angle-integrated energy dependent yields, and the total neutron yield as a function of deuteron energy.

National Library of Australia card number and ISBN 0 642 99764 0

The following descriptors have been selected from the INIS Thesaurus to describe the subject content of this report for information retrieval purposes. For further details please refer to IAEA-INIS-12 (INIS: Manual for Indexing) and IAEA-INIS-13 (INIS: Thesaurus) published in Vienna by the International Atomic Energy Agency.

ANGULAR DISTRIBUTION; BERYLLIUM 9 TARGET; BORON 10; DEUTERON REACTIONS;  
ERRORS; MeV RANGE 01-10; NEUTRON SPECTRA; NEUTRONS; NUCLEAR REACTION  
YIELD; TIME-OF-FLIGHT METHOD

## CONTENTS

	<u>Page</u>
1. INTRODUCTION	1
2. EXPERIMENTAL METHOD	1
2.1 Time-of-Flight Measurement Facility	1
2.2 Background Determination	2
2.3 Data Analysis	3
2.4 Errors	4
3. RESULTS	4
4. CONCLUSIONS	5
5. ACKNOWLEDGEMENTS	5
6. REFERENCES	5
Tables 1-4	Angle-dependent neutron energy spectra from the thick target ${}^9\text{Be}(d,n){}^{10}\text{B}$ reaction, with bombarding deuteron energies of 1.4, 1.8, 2.3 and 2.8 MeV.
Table 5	Calculated maximum neutron energies (MeV) from the ${}^9\text{Be}(d,n){}^{10}\text{B}$ reaction
Table 6	Angular distributions from the thick target ${}^9\text{Be}(d,n){}^{10}\text{B}$ reaction for neutrons with energies above three energy thresholds
Table 7	Total neutron yield above different threshold energies
Figure 1	Pulse height spectra from scintillator
Figure 2	Angle-dependent neutron energy spectra from the ${}^9\text{Be}(d,n){}^{10}\text{B}$ reaction for deuteron energy 1.4 MeV
Figure 3	Angle-dependent neutron energy spectra from the ${}^9\text{Be}(d,n){}^{10}\text{B}$ reaction for deuteron energy 2.8 MeV
Figure 4	Angle-integrated neutron energy spectra
Figure 5	Angular distributions from the thick target ${}^9\text{Be}(d,n){}^{10}\text{B}$ reaction for neutrons with energies greater than 0.25 MeV.

## 1. INTRODUCTION

Some neutronics experiments [Moo et al. 1973] and neutron radiotherapy [Cotterall et al. 1971] require an intense ( $\sim 5 \times 10^{11}$  neutrons  $s^{-1}$ ) source of neutrons. When this source is based on a particle accelerator limited to 3 MV or less, the most prolific neutron sources available are beryllium and lithium bombarded by deuterons. Beryllium is superior to lithium in several respects; for example, its mechanical, chemical and heat conductivity properties permit target construction which withstands prolonged exposure to beams of the order of 200  $\mu A$ . Also, the neutron energy spectrum from the  ${}^9Be(d,n){}^{10}B$  reaction ranges from zero to a few MeV, making this reaction more suitable for some applications than the  ${}^7Li(d,n){}^9Be$  reaction which produces neutrons with energies up to 14 MeV.

Many potential uses of beryllium as a neutron source require that the energy spectrum be well known. The only comprehensive measurement of the  ${}^9Be(d,n){}^{10}B$  reaction in the deuteron energy range 1 to 3 MeV has been made by Inada et al. [1968]. A spectrum measurement made at this laboratory disagreed with that of Inada et al. and motivated the present series of measurements. Although the present measurements use a pulsed time-of-flight technique similar to that of Inada et al., the energy resolution has been improved by using a longer flight path and more advanced analysis. Moreover, the number of neutrons scattered from the floor into the detector have been reduced by using an elevated target facility. Difficulties of interpretation introduced by collimators or shields were thereby avoided.

Only the detailed experimental method and results are presented here. Technical aspects of the time-of-flight facility and comparison of the results with those of Inada et al. will be given in separate publications [Whittlestone 1977a, 1977b].

## 2. EXPERIMENTAL METHOD

### 2.1 Time-of-Flight Measurement Facility

A pulsed deuteron beam from a 3 MV Van de Graaff accelerator was transported by means of two bending magnets to a 3 mm thick, air-cooled beryllium target 5 m above the floor and 6 m from the nearest concrete shield wall. The neutron detector, a 50 mm diameter by 36 mm NE213 scintillator, was mounted 2.26 m from the target. Its lower threshold was set to 0.224 times the mean amplitude of the photopeak from the 0.0596 MeV  $\gamma$ -ray emitted by  ${}^{241}Am$ . At this setting the neutron energy threshold was about 200 keV.

## 2.2 Background Determination

The background could be divided into two parts, the neutrons or  $\gamma$ -rays which were scattered from nearby objects, and those which came directly from the target but which were generated by the residual deuteron beam present when the pulsing system had swept the central core of the beam away from the chopping aperture. The first component was negligible [Whittlestone 1977a], but determination of the second component was complicated by the time dependence of the residual beam.

The background at the low energy end of the spectra was determined by using the scintillator as a proton recoil spectrometer, gated to measure pulse height spectra from different time windows after the beam pulse. The spectrum at any window was the sum of the spectra from two groups of particles: these were neutrons generated during the beam pulse, which will be referred to as 'primary' neutrons, and a combination of neutrons and  $\gamma$ -rays generated by the residual beam. The pulse height spectrum from this last component was the same as the spectrum from the target bombarded by a steady beam, and contained pulses much larger than the pulses from the low energy primary neutrons. It was therefore possible to determine the proportion of primary neutrons in any time window by matching the high pulse height part of the spectrum measured using the time window with the spectrum obtained from a steady beam. The excess counts at the low pulse height end of the window spectrum could be attributed to primary neutrons with energies corresponding to the time range covered by the window.

A typical pulse height spectrum, obtained with a time window set to include primary neutrons with energies between 0.077 and 0.178 MeV, is shown in Figure 1. The deuteron energy ( $E_d$ ) was 2.4 MeV and the angle  $0^\circ$ . Also shown is a pulse height spectrum obtained with no time gating, scaled to match the gated spectrum at the normalisation point indicated. By subtracting the background from the gated spectrum, it was established that 62 per cent of the count was from primary neutrons. A window corresponding to a lower energy, between 0.040 and 0.077 MeV, yielded 26 per cent primary neutrons.

An examination of the time spectrum at  $E_d = 2.4$  MeV and  $0^\circ$  showed that these proportions of primary neutrons could be reproduced by assuming a time-independent background equal to half the count in the channel at 0.073 MeV. Similar measurements and comparisons at  $0^\circ$  showed the same 'recipe' to be valid for the other three deuteron energies used, *i.e.* 1.4, 1.8 and 2.8 MeV. Since it was not feasible to measure time-dependent pulse

height spectra for all four deuteron energies ( $E_d$ ) and seven angles and repeat them, the above recipe was used to calculate the background counts which should be subtracted from the low energy part of all the time-of-flight spectra. The major uncertainty in the recipe is the assumption that the pulse characteristics of the Van de Graaff accelerator did not change from one run to the next. Examination of the time-of-flight spectra indicated that variations of the order 50 per cent in background were possible. This would give rise to an error of about 4 per cent at 0.2 MeV, and about 25 per cent at 0.1 MeV in the energy spectra.

Background correction at the short flight time or high energy end of the spectrum was simpler because the background contribution was small. For example, with a deuteron energy of 2.8 MeV at  $0^\circ$ , the count in three channels above the high energy edge ( $E_{\max} = 7.15$  MeV) was only about 2 per cent of the count in the peak at 6 MeV. The recipe obtained for estimating the background at long flight times was therefore applied to the whole spectrum, ignoring any time dependence. Although this simple approach underestimated the unwanted counts at the high energy end of the spectrum, the error introduced was insignificant. All spectra show a clearly defined edge at high energy corresponding to the  ${}^9\text{Be}(d,n){}^{10}\text{B}$  reaction, leaving  ${}^{10}\text{B}$  in its ground state. The few counts observed above this edge were the result of errors in the background determination and have been set to zero.

### 2.3 Data Analysis

After subtracting the background, the time-of-flight data were unfolded with respect to the time profile of the beam pulse, which was assumed to be the same as that of the gamma flash. An iterative conjugate gradient technique developed by Lang [1977] was used. The code essentially answers the question, 'What would the time spectrum be if the beam pulse profile were confined to one channel?' It is known that, given this ideal time spectrum, say  $S(t)$ , one can generate the time spectrum  $T(t)$  obtained when the beam pulse profile is  $R(t)$ :

$$T(t) = \int_0^\infty R(t-t')S(t')dt' \quad \dots(1)$$

Given the observed time spectrum  $T(t)$  and  $R(t)$  (which in this case is the gamma flash spectrum), the code guesses a spectrum  $S^1(t)$ , then generates a  $T^1(t)$  which it compares with the experimental  $T(t)$ . The difference is used to generate a second  $S^2(t)$  and  $T^2(t)$  and so on, until

$T^n(t)$  agrees with  $T(t)$  within the statistical errors.  $S^n(t)$  is then taken to be the desired unfolded time-of-flight spectrum of the neutrons.

Using this code, the effective time resolution was improved from the 5 ns full width at half maximum of the gamma flash to the 1.5 ns channel width used for measuring the time spectra. Since the flight path was just over 2 m, the energy resolution of the present work was a factor of four better than the resolution of the experiment by Inada et al. [1968]. The energy spectrum was obtained from the unfolded time spectrum in the usual way and, as a final step, the data at low energies were averaged over 50 keV intervals. No significant features of the spectra were lost by this procedure, but the quantity of the data to be tabulated was reduced substantially.

#### 2.4 Errors

The four major sources of error were statistical fluctuations in the time spectra, uncertainties in the detector efficiency, background subtraction and normalisation of the individual spectra to units of neutrons per microcoulomb. In the tabulated data, the errors in the angle-dependent spectra include only the statistical error and the error in the efficiency of the detector. Uncertainties in the background have already been discussed. The additional error introduced by normalisation was 3 per cent. Details of how estimates for the errors in efficiency and normalisation were derived will be given elsewhere [Whittlestone 1977a].

Over most of the energy range, the errors on the individual angle-dependent energy spectra were about 5 per cent. Normalisation to neutron flux per microcoulomb increased the error to about 6 per cent. At low energies the errors were 7 per cent at 0.2 MeV increasing to about 35 per cent at 0.1 MeV.

### 3. RESULTS

The angle-dependent energy spectra are fully presented in Table 1-4 for deuteron energies 1.4, 1.8, 2.3 and 2.8 MeV, and angles 0, 30, 45, 60, 90, 120 and 150°. To simplify comparison with the results of Inada et al. [1968], these data have been expressed as neutron fluences at the detector for a target-detector separation of 1 m, and quoted in units of neutrons  $\text{MeV}^{-1} \text{cm}^{-2} \mu\text{C}^{-1}$ . Spectra at 0, 30, 60 and 150° for deuteron energies 1.4 and 2.8 MeV have been plotted in Figures 2 and 3.

The last two columns in Tables 1-4 give the value and error of the yield ( $\text{MeV}^{-1} \mu\text{C}^{-1}$ ) formed by integrating the flux over a sphere. This result is also plotted in Figure 4.



For completeness, the maximum neutron energy expected at each angle and deuteron energy has been calculated using the  $Q$  value for the ground state transition as quoted by Lauritsen & Ajzenberg-Selove [1966]. These energies are given in Table 5.

Table 6 gives the angular distributions of neutron fluences for the  $\text{Be}(d,n)$  reaction, formed by integrating the angle-dependent energy spectra over energy above energy thresholds of 0.075, 0.25 and 0.95 MeV. The angular distribution with neutron energy threshold 0.25 MeV has been plotted in Figure 5. Finally, the angular distributions have been integrated to give the total neutron yield above the same three neutron energy thresholds. These yields are given in Table 7, which also gives the total yield for neutrons of all energies, estimated by extrapolating plots of the Table 6 data to zero neutron energy.

#### 4. CONCLUSIONS

A comprehensive measurement of the angle-dependent neutron energy spectra from the  ${}^9\text{Be}(d,n){}^{10}\text{B}$  reaction has been made for deuteron energies between 1.4 and 2.8 MeV. The spectra are accurate to about 6 per cent above a neutron energy of 0.2 MeV, and have an energy resolution limited by the channel width, which is 0.3 MeV at a neutron energy of 7 MeV.

Although the experiment was set up to measure spectra of neutrons with energies greater than 0.2 MeV, it was established that there is a significant number of neutrons at 0.1 MeV. There is, therefore, a need for a measurement of the neutron energy spectra in the range 0 to 0.2 MeV.

#### 5. ACKNOWLEDGEMENTS

The author is grateful for discussions with Dr. A.I.M. Ritchie. The assistance of the technical staff associated with the Van de Graaff accelerator has also been most valuable.

#### 6. REFERENCES

- Cotterall, M., Rogers, C.C., Thomlinson, R.H. & Fields, S.B. [1968] - Brit. J. Radiol., 44:603.
- Inada, T., Kawachi, K. & Hiramoto, T. [1968] - J. Nucl. Sci. Tech., 5:22.
- Lang, D. [1977] - AAEC/E398 (in press).
- Lauritsen, T. & Ajzenberg-Selove, F. [1966] - Nucl. Phys., 78:111.
- Moo, S.P., Rainbow, M.T. & Ritchie, A.I.M. [1973] - J. Nucl. En., 27:753.
- Whittlestone, S. [1977a] - AAEC/E report (in preparation).
- Whittlestone, S. [1977b] - J. Phys. D - submitted for publication.

TABLES 1-4  
ANGLE-DEPENDENT NEUTRON ENERGY SPECTRA FROM THE THICK TARGET  
 $^9\text{Be}(d,n)^{10}\text{B}$  REACTION, WITH BOMBARDING DEUTERON ENERGIES  
OF 1.4, 1.8, 2.3 AND 2.8 MeV.









TABLE 5  
CALCULATED MAXIMUM NEUTRON ENERGIES (MeV)  
EXPECTED FROM THE  ${}^9\text{Be}(d,n){}^{10}\text{B}$  REACTION

Deuteron Energy (MeV)	Angle (degrees)	0	30	45	60	90	120	150
1.4		5.71	5.60	5.49	5.33	4.98	4.65	4.42
1.8		6.13	6.01	5.86	5.68	5.27	4.89	4.62
2.3		6.64	6.50	6.33	6.12	5.63	5.19	4.88
2.8		7.15	6.99	6.79	6.55	6.00	5.49	5.15

TABLE 6  
ANGULAR DISTRIBUTIONS FROM THE THICK TARGET  ${}^9\text{Be}(d,n){}^{10}\text{B}$   
REACTION FOR NEUTRONS WITH ENERGIES ABOVE THREE  
NEUTRON ENERGY THRESHOLDS

Angle (degrees)		0	30	45	60	90	120	150
Deuteron Energy (MeV)	Neutron Threshold Energy (MeV)	neutrons $\text{cm}^{-2} \mu\text{C}^{-1}$ at 100 cm						
		1.4	0.075	5924	5657	5257	4785	4256
	0.25	4571	4366	4085	3705	3249	3622	3728
	0.95	2283	2829	2937	2790	2622	3137	3269
1.8	0.075	13086	7823	7508	8102	7628	10598	9111
	0.25	10933	6377	6053	6544	6125	8456	7186
	0.95	4501	3751	4104	4621	4394	6281	5585
2.3	0.075	25365	20028	15981	14373	12886	12301	12483
	0.25	21748	16822	13081	11654	10275	9553	9769
	0.95	14524	11778	9519	8537	7362	6722	6886
2.8	0.075	45946	31650	25227	22580	19420	17183	17528
	0.25	39385	26530	20422	18161	15333	13357	13595
	0.95	29396	19063	14753	13296	11280	9408	9355



TABLE 7

TOTAL NEUTRON YIELD ABOVE DIFFERENT THRESHOLD ENERGIES

Deuteron Energy (MeV)	1.4	1.8	2.3	2.8
Threshold Energy (MeV)	Yield (neutrons $\mu\text{C}^{-1}$ ) $\div 10^8$			
0.075	6.016	10.92	17.60	26.68
0.25	4.592	8.761	14.20	21.33
0.95	3.647	6.220	10.12	15.37
0 (extrapolated values)	7.2	12.3	20.0	30.0

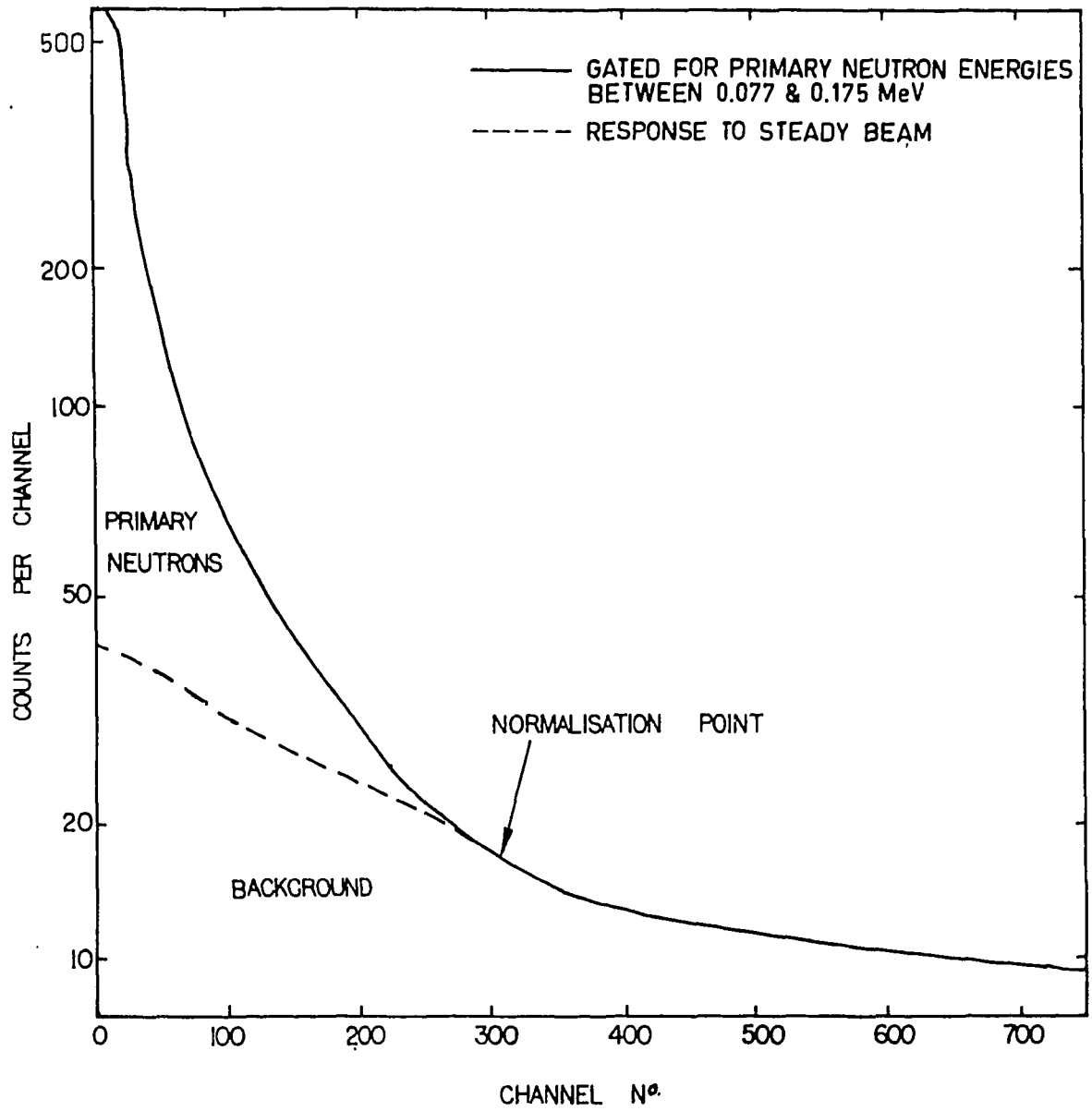


FIGURE 1. PULSE HEIGHT SPECTRA FROM SCINTILLATOR

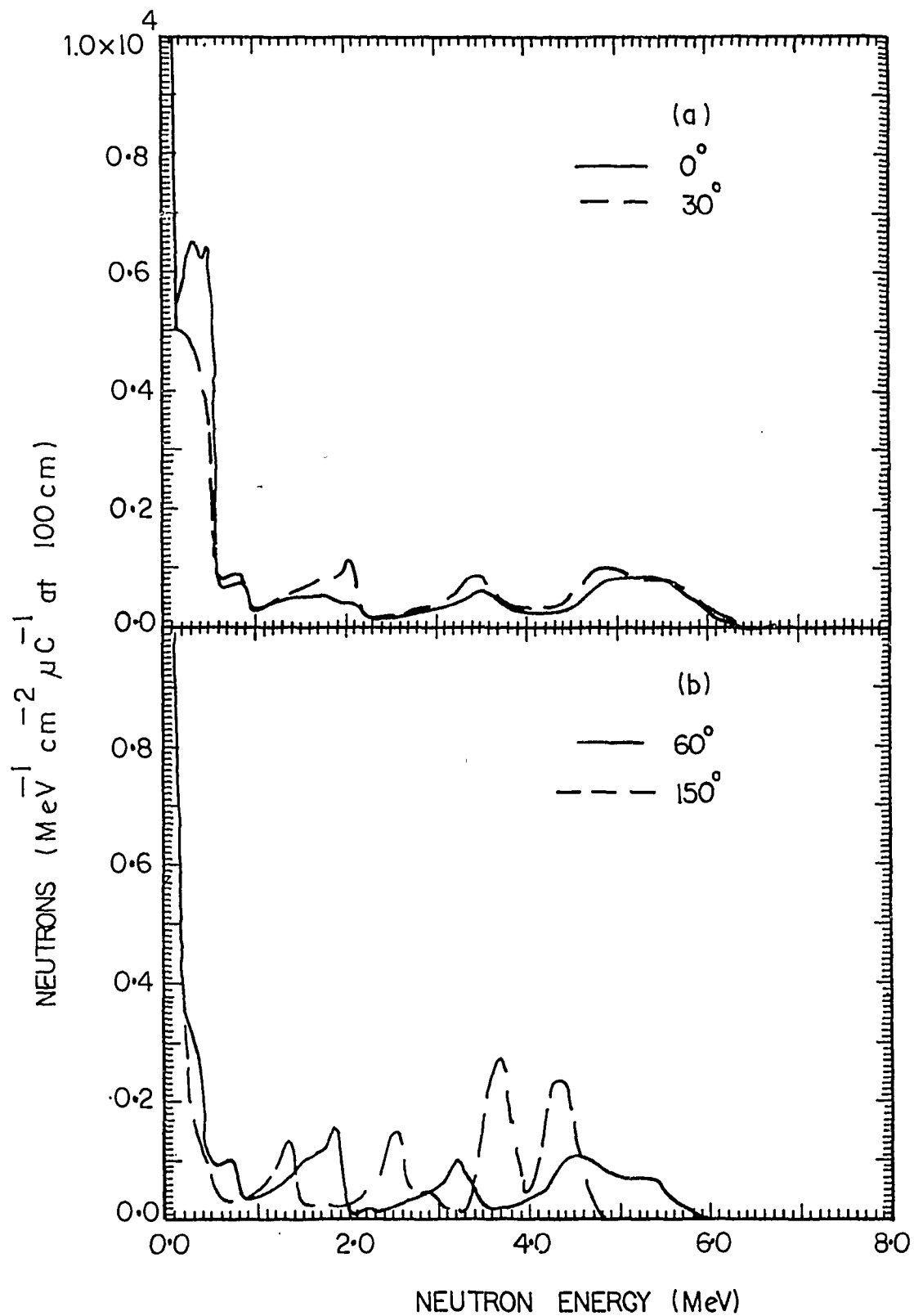


FIGURE 2. ANGLE-DEPENDENT NEUTRON ENERGY SPECTRA FROM THE  ${}^9\text{Be}(d,n){}^{10}\text{B}$  REACTION FOR DEUTERON ENERGY 1.4 MeV

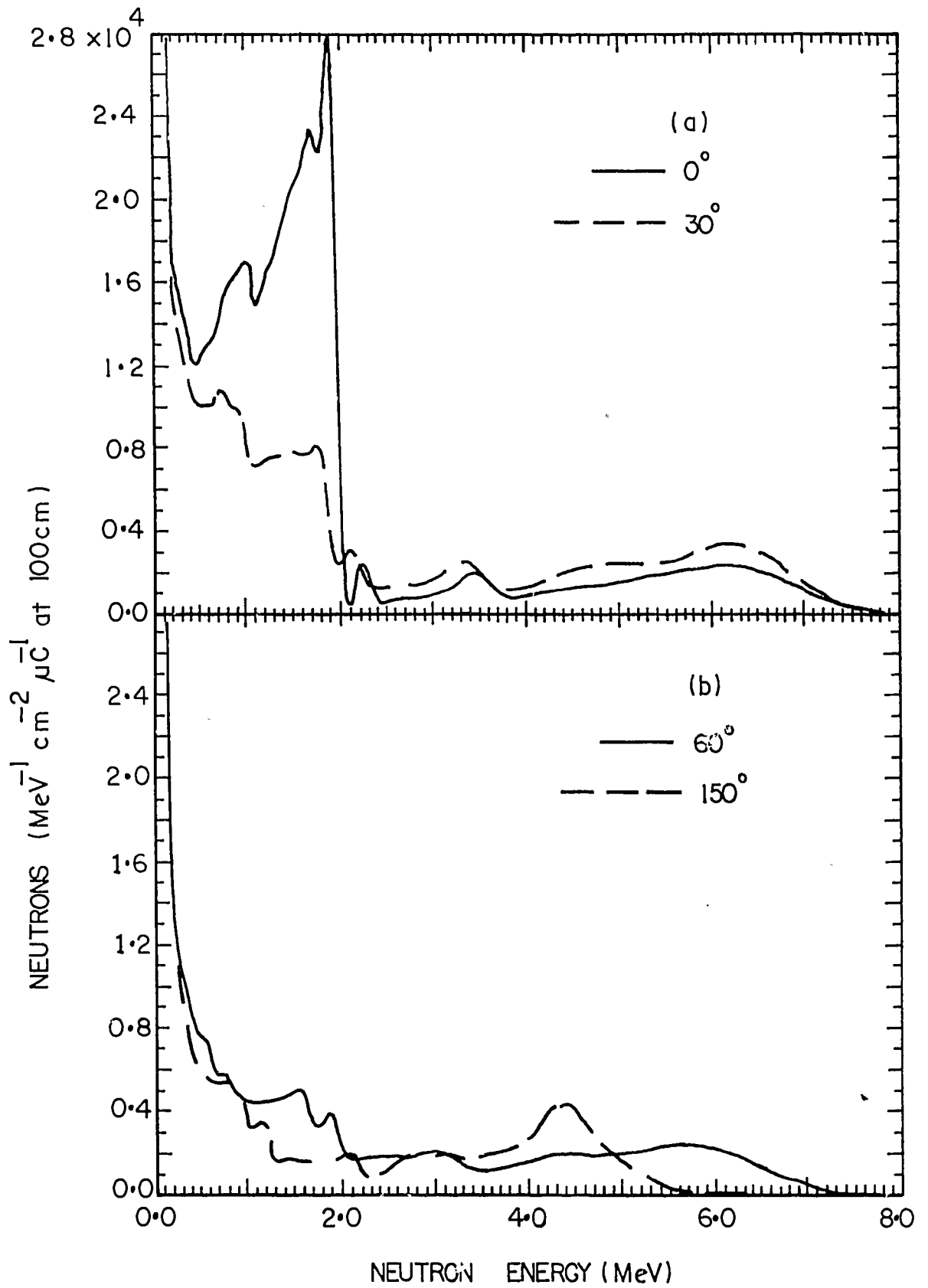


FIGURE 3. ANGLE-DEPENDENT NEUTRON ENERGY SPECTRA FROM THE  ${}^9\text{Be}(d,n){}^{10}\text{B}$  REACTION FOR DEUTERON ENERGY 2.8 MeV

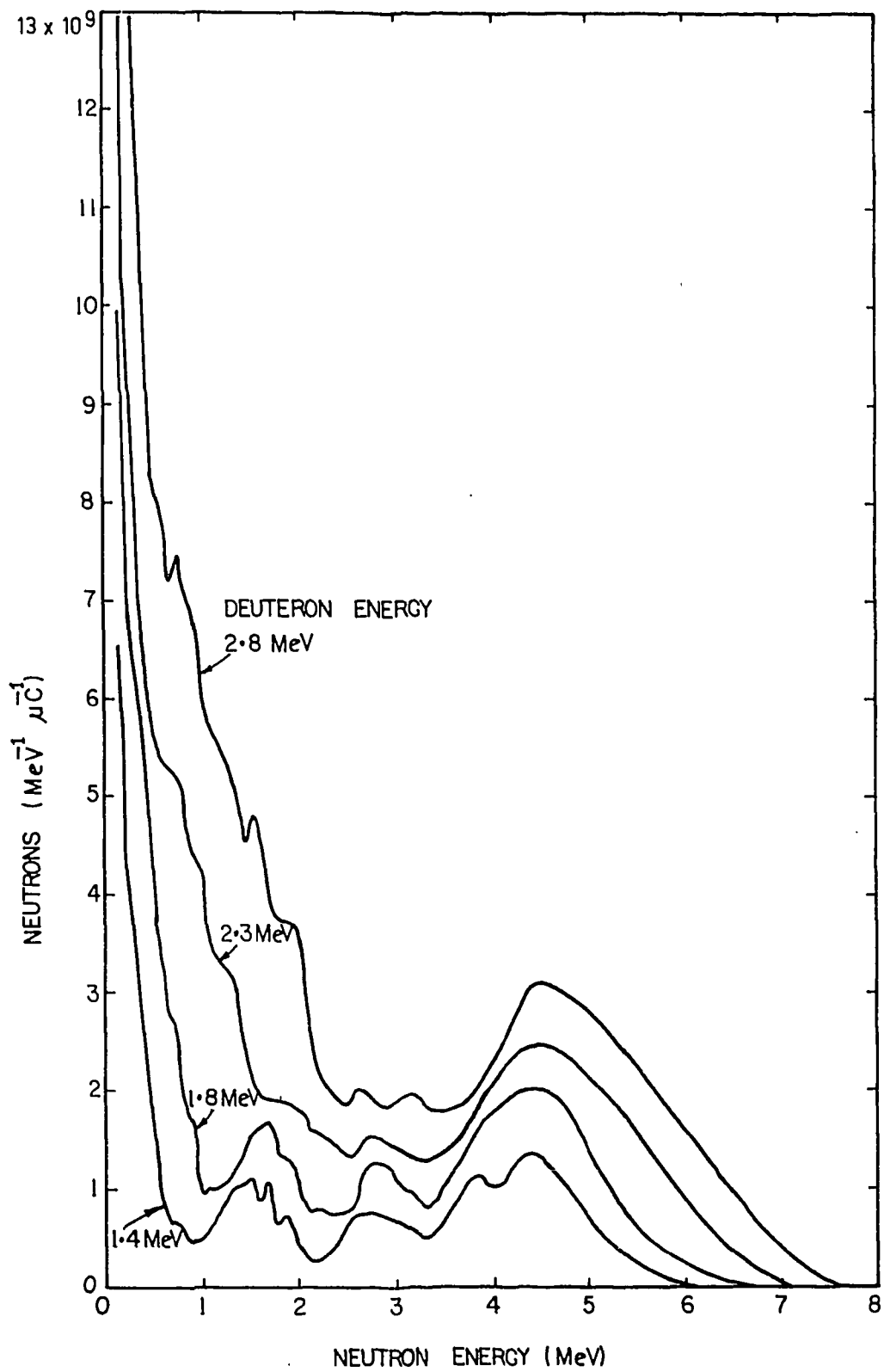


FIGURE 4. ANGLE-INTEGRATED NEUTRON ENERGY SPECTRA

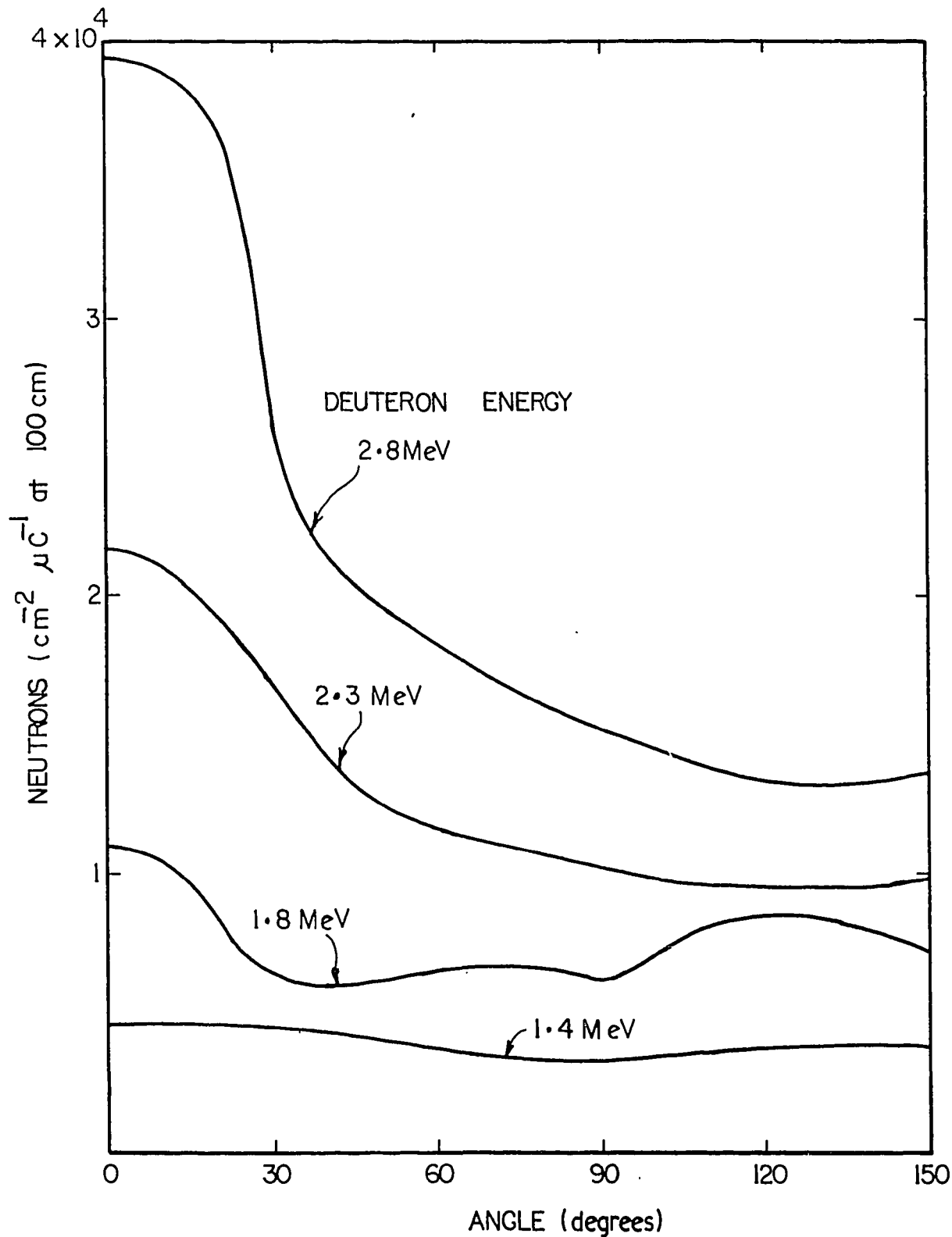


FIGURE 5. ANGULAR DISTRIBUTIONS FROM THE THICK TARGET  ${}^9\text{Be}(d,n){}^{10}\text{B}$  REACTION FOR NEUTRONS WITH ENERGIES GREATER THAN 0.25 MeV